Dalton Transactions

Accepted Manuscript

ROYAL SOCIETY OF CHEMISTRY

www.rsc.org/dalton

Cite this: DOI: 10.1039/c0xx00000x

www.rsc.org/xxxxxx

ARTICLE TYPE

Sputtering-deposition of Ru nanoparticles onto Al_2O_3 modified with imidazolium ionic liquids: Synthesis, characterisation and catalysis

Lucas Foppa,[a] Leandro Luza,[a] Aitor Gual,[a] Daniel E. Weibel,[a] Dario Eberhardt,[b] Sérgio R. Teixeira[b] and Jairton Dupont[a,c*]

Received (in XXX, XXX) XthXXXXXXXXX 20XX, Accepted Xth XXXXXXXXX 20XX
DOI: 10.1039/b000000x

Well-distributed Ru nanoparticles (Ru-NPs) were produced over Al_2O_3 supports modified with covalently anchored imidazolium ionic liquids (ILs) containing different anions and cation lateral alkyl chain lengths by simple sputtering from a Ru foil. These Ru-NPs were active catalysts for the hydrogenation of benzene. Furthermore, depending on the nature of the IL used to modify the support (hydrophilic or hydrophobic), different catalytic behaviours were observed. Turnover numbers (TON) as high as 27,000 with a turnover frequency (TOF) of 2.73 s^{-1} were achieved with Ru-NPs of 6.4 nm supported in Al_2O_3 modified with an IL containing the $N(SO_2CF_3)_2^-$ anion, whereas higher initial cyclohexene selectivities (ca. 20% at 1% benzene conversion) were attained for Ru-NPs of 6.6 nm in the case where Cl^- and BF_4^- anions were used. Such observations highly suggest that thin layers of IL surround the NPs surface, modifying the reactivity of these catalytic systems. These findings open a new window of opportunity in the development of size-controlled Ru-NPs with tuneable reactivity.

Introduction

Transition metal nanoparticles (M-NPs) are currently used as effective catalysts for hydrogenation processes in which homogeneous and traditional heterogeneous catalysts are less efficient.[1,2,3,4] Modern soluble M-NPs are commonly synthesised by chemical methods, which involve the reduction of metallic salts or the decomposition of organometallic complexes in the presence of stabilising agents.[1,2,5,6,7,8] Recently, the use of sputtering-deposition techniques was revealed as an interesting alternative for the synthesis of soluble M-NPs with cleaner surfaces under mild conditions and easier control of their size and shape by appropriate tuning of sputtering conditions.[9, 10,11,12,13,14,15] This approach allows the rapid synthesis of M-NPs catalysts by deposition of metals on support surfaces or the fast generation of M-NPs in solution using low volatility liquids such as silicones, triglycerides, and ILs. This method is widely applied for the formation of thin (nanosized) films onto supports[16]; however, it is limited since it is extremely difficult to prepare uniformly distributed M-NPs on solid catalytic supports.[17] Recently, our group reported the synthesis of Pd-NPs by sputtering-deposition of Pd-foil using Al_2O_3 and SiO_2 modified with imidazolium ILs as supports.[14, 18] These NPs were revealed as an active catalyst for the hydrogenation of dienes, and displayed improved activities and selectivities than those obtained using Pd-NPs synthesised by conventional decomposition of organometallic precursors.

Among the various types of agents for stabilising soluble M-NPs, ILs[19] are extensively employed owing to their higher efficiency in hydrogenation processes.[6,20] Recently, the use of supported ionic liquid phase (SILP) is receiving growing interest since the ILs surface area is increased relative to its volume and the substrate can readily diffuse to the catalysts, overcoming the mass transfer limitations produced by the high viscosity of the IL.[21, 22] The SILP system uses much smaller amounts of IL than those required under liquid/liquid biphasic conditions, and this behaviour is of crucial importance for reactions involving gases with poor solubility in IL (for example H_2 and CO). Therefore, catalysis using SILP as a support combines the positive effects of IL on the catalytic performance with the high stability of the catalysts, good diffusion of the reactants, and easy product separation displayed by heterogeneous catalysts. The most widely used ILs in SILP applications are imidazolium ILs, which combine the high solvation power of polar species with their weak coordination strength, making them suitable for reactions with electrophilic catalysts.[23,22] Silica is the most widely used support for the immobilisation of M-NPs due to their high surface area and the presence of OH, which facilitate the anchoring of stabilising agents, whereas the use of other supports has scarcely been reported.[24] To the best of our knowledge, the use of alumina (Al_2O_3)-based supports in an SILP system, which offer higher stability at higher pH, has been scarcely explored until now.[14]

Here, we report the synthesis and characterisation of a series of imidazolium ILs covalently immobilised onto Al_2O_3 surfaces. Ru-NPs were uniformly distributed on these supports by a sputtering-deposition technique. Furthermore, the hydrogenation of benzene was used to probe the surface properties of these new SILP Ru-NPs. The hydrogenation of benzene was chosen as a benchmark reaction since it is a structure-sensitive reaction.[4] Moreover, the partial hydrogenation of aromatics, such as benzene, is of interest for the treatment of diesel to obtain low-aromatic content diesel fuels, the hydrogenation of aromatic

polymers to produce new materials and the production of fine chemicals.[4]

Results and Discussion

Synthesis and characterisation of the Al_2O_3 modified supports

The **M1-M4** hybrid alumina supports have been prepared as already described[14] and their physicochemical properties were included in order to compare the data with supports **B1-B4**. It is expected that the replacement of the methyl group in **M1-M4** for the *n*-butyl side chain (**B1-B4**) will increase the non-polar domains of the hybrid materials.

Thus, the **M1** and **B1** supports were synthesised by respectively reacting 1-methyl-3-(trimethoxysilylpropyl)-imidazolium chloride (**1**) and 1-*n*-butyl-3-(trimethoxysilylpropyl)-imidazolium chloride (**2**) with the hydroxyl groups of the alumina surfaces and their further ion-exchange treatment by modified literature procedures[25] was carried out in order to obtain the **M2-M4** and **B2-B4** supports containing counter-ions NTf_2^-, PF_6^- and BF_4^-, respectively (Scheme 1).

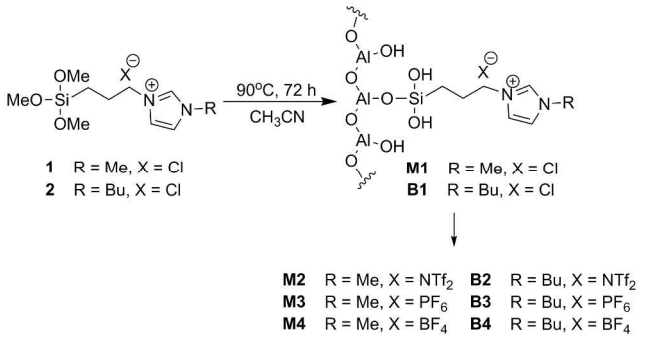

Scheme 1. Synthesis of **M1**–**M4** and **B1**–**B4** supports.

^{13}C CP-MAS NMR of the supports **M1-M4** displayed four sets of up-field broad peaks (10, 25, 36 and 52 ppm) which could be assigned to the propylene and methylene functions, whereas the resonances at 123 and 136 ppm were assigned to the three imidazolium carbon atoms (Figure 1). ^{13}C CP-MAS NMR of the supports **B1-B4** displayed seven sets of up-field broad peaks (11, 12, 19, 25, 32, 49 and 52 ppm) which could be assigned to the propylene and butylene functions, whereas the resonances at 123 and 136 ppm were assigned to the three imidazolium carbon atoms (Figure 1). Thus, these NMR signals confirmed the presence of the unaltered imidazolium ILs in **M1-M4** and **B1-B4** supports. It should be noted that no signal attributed to the methoxy leaving groups (65 ppm) of the silane function was observed, confirming that the trimethoxy-silane group effectively reacted with the hydroxyl groups of the Al_2O_3 surface under our reaction conditions.

FT-IR analysis of **M1-M4** and **B1-B4** supports showed C=N stretching vibration bands of the imidazolium rings and C−H stretching vibrations bands of the alkyl groups at 1635 and 2950 cm^{-1}, respectively (Figure 2). Therefore, these IR signals also confirmed the presence of the unaltered imidazolium ILs in **M1-M4** and **B1-B4** supports. Furthermore, FT-IR analysis of the supports **M1-M4** and **B1-B4** displayed signals attributed to NTf_2^- (1058, 1145, 1220 and 1350 cm^{-1}), PF_6^- (741 and 841 cm^{-1}) and BF_4^- (763, 1039 and 1061 cm^{-1}), respectively, thus confirming the efficiency of the Cl^- exchange procedure[26,27].

Table 1. Characterisation of the supports.

Support	S_{BET}/ m^2g^{-1}[a]	*Pore Volume* /$cm^2\ g^{-1}$[a]	*Pore Diameter* / *nm*[a]	*Organic Content*[b]/ *mmol IL* g^{-1}
Al_2O_3	195	0.47	8.0	-
M1	134	0.31	6.9	0.46
M2	127	0.28	6.6	0.36
M3	125	0.30	7.0	0.39
M4	80	0.20	7.1	0.38
B1	143	0.34	7.0	0.38
B2	147	0.33	6.9	0.27
B3	139	0.33	7.5	0.31
B4	107	0.23	6.7	0.35

[a] Determined using a Tristar 3020 Micromeritics equipment. The specific surface areas were determined by the BET multipoint method and the average pore size was obtained by BJH method; [b] Calculated on the basis of the nitrogen content determined by elemental analysis using a CHN Perkin Elmer M CHNS/O Analyzer, model 2400.

Nitrogen physisorption analysis revealed type-IV-like isotherms with pore diameters of 6.6 to 8.0 nm for the unmodified Al_2O_3 and **M1-M4** and **B1-B4** supports (Table 1). The **M1-M4** and **B1-B4** supports displayed lower surface areas and pore volumes than the unmodified Al_2O_3, indicating that the ILs were filling the pores. Similar behaviour was observed for the ILs covalently supported on SiO_2.[28]

Elemental analysis revealed that **M2-M4** and **B2-B4** supports displayed slightly lower amounts of IL than the **M1** and **B1** supports, which suggests that IL was removed from these supports during the Cl^- exchange step (Table 1). A comparison of the data displayed between the supports reveals that **B1-B4** (with a *n*-butyl group) supports displayed higher surface areas and pore volumes with slightly larger pore diameters than **M1-M4** (with a methyl group) supports, which could be directly related to the fact that **B1-B4** supports contained lower IL amounts than **M1-M4** supports.

The effect of the Cl^- exchange on the **M1-M4** and **B1-B4** support structure was investigated by ^{29}Si CP-MAS NMR analysis (Figure 3). The spectra of **M1** and **B1** displayed the typical signals of silicon atoms attached to one carbon atom and to the alumina surface at −46 and −55 ppm assigned to the **T1** (20% and 60%, respectively) and **T2** (80% and 40%, respectively) species.[29] After the Cl^- exchange, a new signal at −65 ppm appeared on the **M2-M4** and **B2-B4** supports, which was attributed to the formation of **T3** species, suggesting that rearrangement processes were operating under the reaction conditions of the Cl^- exchange step. This behaviour could be ascribed to the formation of hydrogen fluoride by hydrolysis of the fluorine-based anions.[30] This effect was much more pronounced for the supports containing the anions PF_6^- and BF_4^- (30-40% and 50% of **T3**, respectively), which decomposed more easily than NTf_2^- (10% of **T3**) (Figure 3). A comparison of the data displayed between the supports reveals that **B1-B4** (with an *n*-butyl group) displayed more uniform distributions of the IL onto the Al_2O_3 than **M1-M4** (with a methyl group). This effect could be directly ascribed to the higher steric hindrance produced by the *n*-butyl group compared with the methyl group.

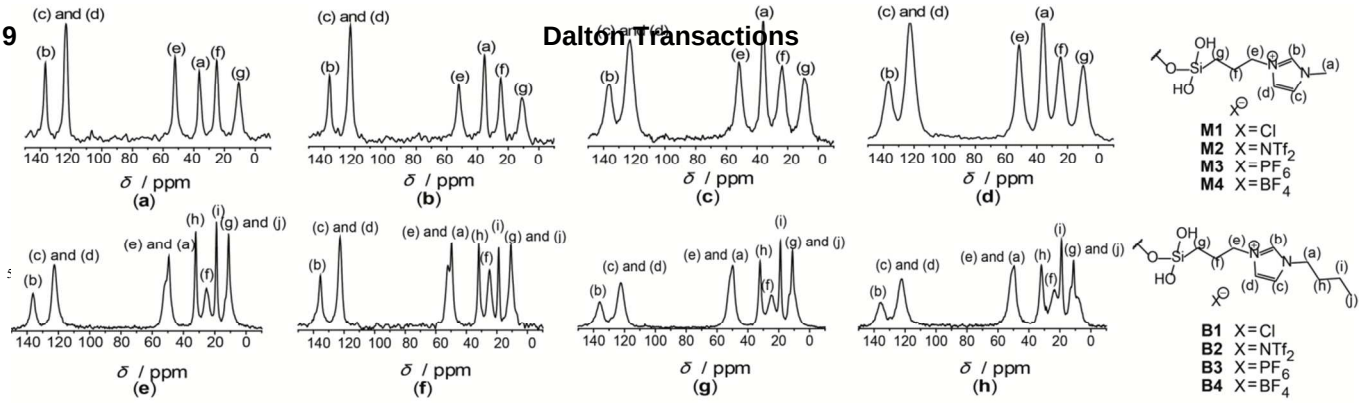

Figure 1. ^{13}C CP-MAS NMR spectra of (a) **M1**, (b) **M2**, (c) **M3** and (d) **M4**, (f) **B1**, (g) **B2**, (h) **B3** and (i) **B4**. ^{13}C NMR (a)-(d) were previously described in ref. 14.

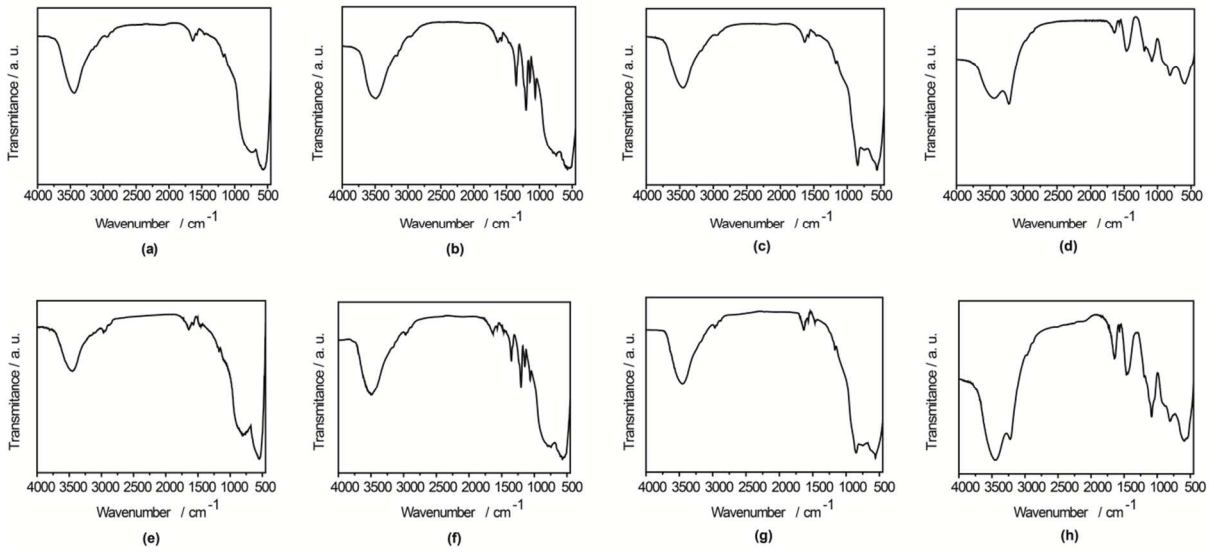

Figure 2. FT-IR spectra of (a) **M1**, (b) **M2**, (c) **M3** and (d) **M4**, (e) **B1**, (f) **B2**, (g) **B3** and (h) **B4**. FT-IR (a)-(d) were previously described in ref. 14.

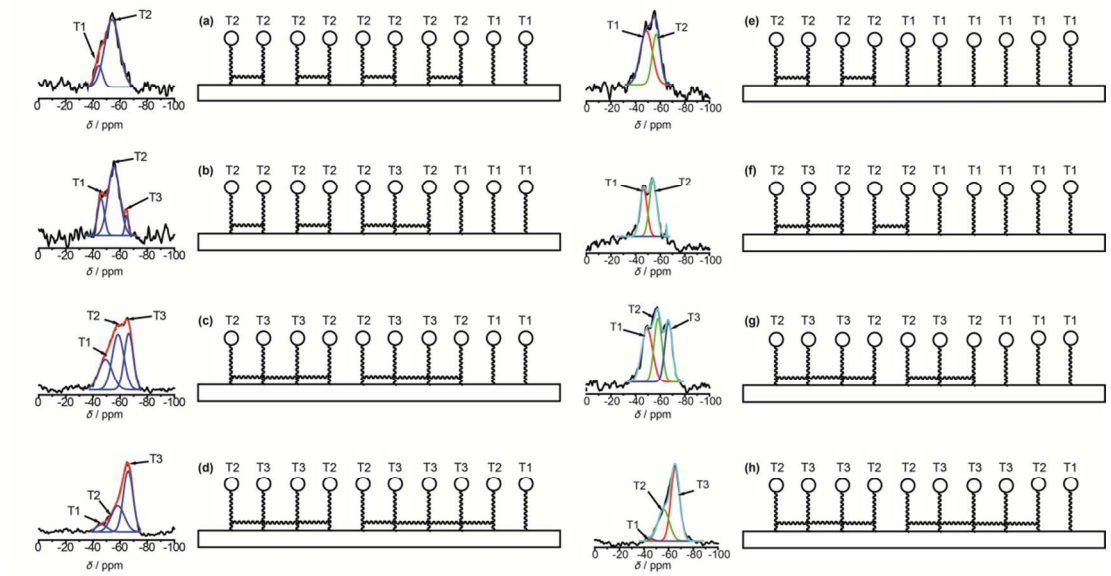

Figure 3. ^{29}Si CP-MAS NMR spectra of (a) **M1**, (b) **M2**, (c) **M3** and (d) **M4**,(e) **B1**, (f) **B2**, (g) **B3** and (h) **B4**. ^{29}Si NMR (a)-(d) were previously described in ref. 14.

M1-M4 and **B1-B4** supports stability was also tested by means of TGA (thermogravimetric analysis) (Figures S1 and S2 on Supporting Information). IL decomposition temperature was observed in the range between 300-450°C, which makes these materials suitable for a wide range of applications in catalysis. Similar decomposition temperatures were observed for the case supported ionic liquids synthesised by impregnation of imidazolium salts onto Al_2O_3 supports.[31]

Therefore, **M2** and **B1-B4** were selected as suitable supports for the deposition of Ru-NPs by the sputtering technique in order to study the effect of the structure and distribution of the ILs covalently anchored onto the Al_2O_3 on the Ru-NPs physical and catalytic properties.

Sputtering deposition of Ru-NPs onto Al_2O_3-based supports

Ru-NPs were obtained on the above-mentioned supports by magnetron-sputtering using a power of 145 W for 10 min. The catalysts were then characterised. Metal content determination by X-Ray Fluorescence (XRF) analysis revealed values of Ru content between 0.8 and 1.5% (w/w) (see Table 2). Dark-Field Transmission Electron Microscopy (DF-TEM) revealed that small nanoparticles (ca. 4.8-7.7 nm) with narrow size distributions (ca. 1.3-1.8 nm) were obtained (see Table 2 and Figure 4). It should be noted that the catalyst with the lowest metal content (Ru/Al_2O_3) also displayed the smallest nanoparticle mean diameter (4.8 nm) and the catalyst containing the highest metal concentration (Ru/**B3**) displayed the largest one (7.7 nm), whereas the rest of the catalysts bearing metal contents between 1.0 and 1.3% (w/w) displayed nanoparticles with similar sizes (6.4-6.6 nm).

This behaviour suggested that the metal nanoparticle size obtained under similar sputtering conditions is mainly governed by the nature of the support and by the amount of metal deposited (sputtering deposition conditions) onto the support, and no significant influence of the IL lateral alkyl chain or of the nature of the counter-anion was observed. This is in contrast to that which was observed in net ILs in which the nature of anion also plays an important role on the size of M-NPs prepared by sputtering deposition.[10]

Table 2. Characterisation of the Ru-NPs supported onto Al_2O_3, **M2** and **B1-B4**.

Ru-NPs	*NPs Φ [a] / nm*	*Ru content [b] / %(w/w)*
Ru/Al_2O_3	4.8 ± 1.3	0.8 ± 0.1
Ru/**B1**	6.6 ± 1.5	1.1 ±0.1
Ru/**M2**	6.6 ± 1.4	1.0 ±0.1
Ru/**B2**	6.4 ± 1.4	1.3 ± 0.1
Ru/**B3**	7.7 ± 1.8	1.5 ±0.2
Ru/**B4**	6.6 ± 1.4	1.0 ±0.1

[a] Determined by measuring at least 300 nm NPs of the dark-field TEM micrographs; [b] Determined by X-Ray Fluorescence Analysis (XRF).

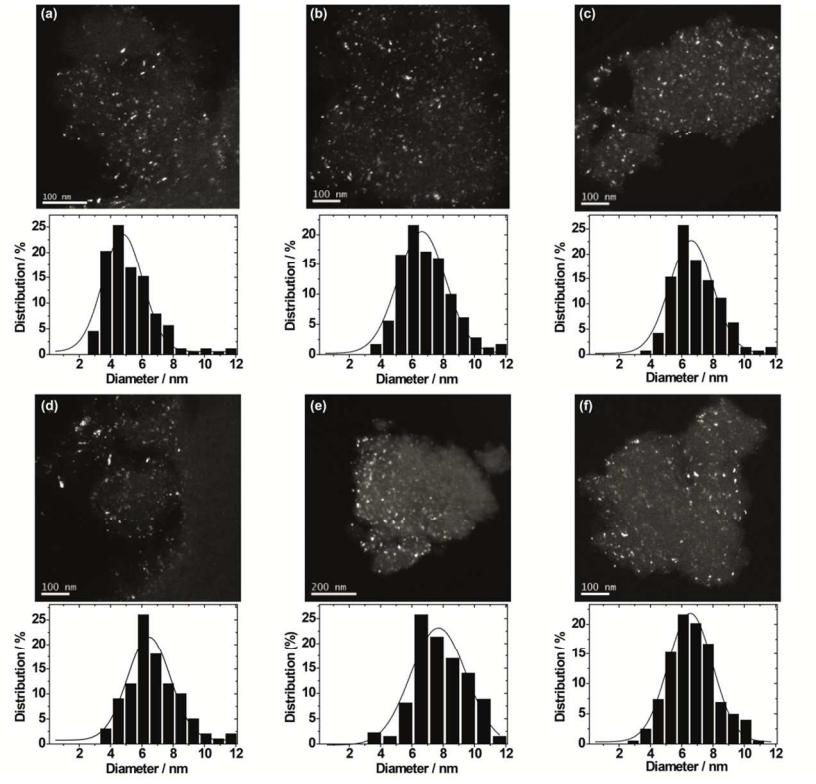

Figure 4. Dark Field Transmission Electron Microscopy of the catalysts Ru/Al_2O_3 (a), Ru/**B1** (b), Ru/**M2** (c), Ru/**B2** (d), Ru/**B3** (e) and Ru/**B4** (f).

For comparative purposes, Ru-NPs supported onto Al_2O_3 with higher metal content (ca. 3% (w/w)) were synthesised by magnetron-sputtering and characterised by X-Ray Diffraction (XRD) and X-Ray Photoelectron Spectroscopy (XPS). Analysis of the selected region of the XRD patterns of Al_2O_3 and of the Ru-NPs immobilised onto Al_2O_3 revealed the appearance of a signal at 44° due to the presence of Ru(0)-hcp NPs, although the metal content was probably not high enough to provide a clear peak even for high counts.

Additionally, samples with a metal content of 3% (w/w) prepared by magnetron-sputtering were compared to catalysts with similar metal content obtained by hydrogen reduction of Ru(Me-allyl)$_2$(COD) (general procedure described in Supporting Information) using XPS. First, the quantification of the survey XPS spectra shows that the Ru/Al ratio is more than six times higher when the Ru-NPs were synthesised by magnetron-sputtering (0.2) compared to the colloidal method (0.03).

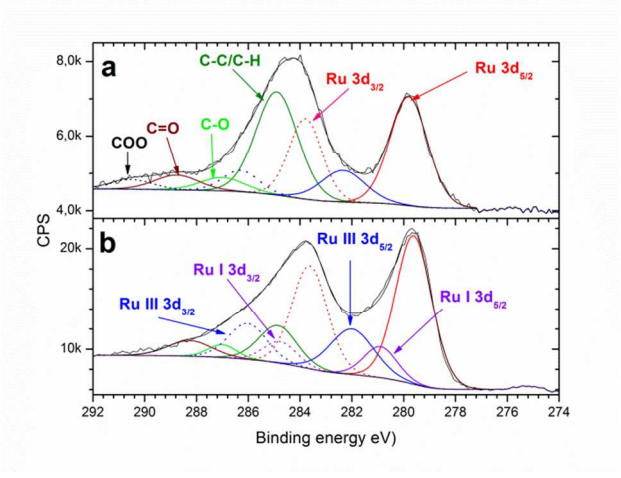

Figure 5. Selected region of the XPS spectra of the Ru-NPs immobilised onto Al_2O_3: synthesised by reduction of Ru(Me-allyl)$_2$(COD) (a), and synthesised by magnetron-sputtering (b).

Furthermore, Ru 3d and C 1s XPS spectra were obtained and analysed (see Figure 5). C 1s and Ru 3d peaks strongly overlap and they were not sufficiently well resolved under our experimental conditions. However, the relative quantification of both contributions shown in Figure 5 can be determined by peak fittings. The fitting shows that the C/Ru ratio decreased from 5.0 when the Ru-NPs were synthesised by reduction of Ru(Me-allyl)$_2$(COD) to 0.7 when they were prepared by magnetron-sputtering. These results, together with the information obtained from elemental analysis, demonstrate the benefit of the magnetron-sputtering method to allow the deposition of a much higher concentration of Ru-NPs in the surface region of the support, in contrast to the catalysts synthesised by conventional chemical methods. From Figure 5, it is also possible to observe a higher surface oxidation of the Ru-NPs. Data suggest that about 64% and 24% of the Ru-NPs were oxidised after preparation by magnetron-sputtering and by the reduction of Ru(Me-allyl)$_2$(COD), respectively.

Ru-NPs catalysed the hydrogenation of benzene

These novel nanocatalysts prepared by the sputtering technique were tested in the hydrogenation of benzene under 4 bar of H_2 at 75°C, since this reaction is commonly used as a benchmark test for evaluation of the activity and selectivity of Ru-NPs.[4]

Table 3 displays the activities obtained in terms of TON and TOF. The following order of activity was observed: Ru/**B2** > Ru/**B3** > Ru/**M2** ≈ Ru/Al_2O_3 > Ru/**B4** > Ru/**B1**. (Table 3, Entries 1-6). Catalyst Ru/**B2**, whose support contains the covalently anchored IL with the anion NTf_2^- and an *n*-butyl chain attached to the imidazolium ring of the cation, afforded the highest activity. With this catalyst, TONs of 27000 (moles benzene (**BEN**)/mol surface Ru) were achieved at high conversions (ca. 100%). Compared to the non-modified support, Ru/**B2** as well as Ru/**B3** displayed higher turnover frequencies (Table 3, Entries 1, 4 and 5). Additionally, Ru/**B2** displays a slightly higher activity with respect to Ru/**M2**, in which the imidazolium cation of the IL contains a methyl side chain (Table 3, Entries 3 and 4). These TOF values are much higher than those already described in the literature for similar systems using Ru-NPs synthesized from organometallic precursors, the nanoparticles being dispersed in pure BMI.PF_6 IL during reaction (ca. 0.0056 s^{-1} at 75°C and 4 bar H_2).[4, 32]

Table 3. Ru-NPs catalysed hydrogenation of benzene.

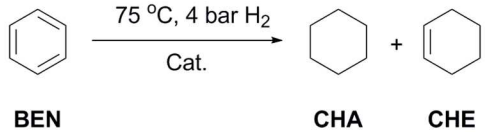

Cat. = Ru/Al_2O_3, Ru/**M2** and Ru/**B1-B4.**

Entry[a]	*Catalyst*	***BEN*** *Conv./ %* [b]	*TON* [b,c]	*TOF/s*$^{-1}$ [b,d]
1	Ru/Al_2O_3	25.2	9160	2.55
2	Ru/**B1**	6.7	2160	0.59
3	Ru/**M2**	24.6	9160	2.55
4	Ru/**B2**	34.8	9600	2.73
5	Ru/**B3**	44.5	9260	2.62
6	Ru/**B4**	11.3	4000	1.09
7[e]	Ru/Al_2O_3 - BMI.NTf_2	2.7	980	0.28
8[e]	Ru/Al_2O_3 - BMI.PF_6	1.5	550	0.12
9[e]	Ru/Al_2O_3- BMI.BF_4	11.4	4150	1.14

[a] Reaction conditions: benzene (**BEN**) (2.64 g, 34 mmol), Ru-catalyst (50 mg), 75°C and 4 bar of H_2. Conversion determined by GC-FID; [b] Calculated for 1 h reaction time; [c] TON=converted moles of benzene (**BEN**)/moles of Ru on the surface of the NP; [33] [d] TOF obtained from TON *vs.* time slope; [e] Imidazolium ILs (ca. 0.3 *mmol IL g cat.* $^{-1}$) were dispersed by simple impregnation onto the Ru/Al_2O_3 catalyst.

Cyclohexene (**CHE**) selectivity as a function of the benzene (**BEN**) conversion was also monitored during the experiments (See Figure 6). Even if selectivity values attained are not as high as those reported for similar supported Ru catalysts modified with more hydrophilic dycianamide-containing ILs (70% at very low conversion ca. 3%),[34, 35] our experiment show that common ILs covalently bonded to the support can significantly increase the amount of cyclohexene obtained.

It was observed that the catalysts whose supports contain Cl^- and BF_4^- as the counter-ion of the supported IL (Ru/**B1** and Ru/**B4**, respectively) produced much higher selectivities towards the partially hydrogenated product (up to 20% at low benzene conversions) compared to the other SILP catalysts or the Ru/Al_2O_3 catalyst, despite being less active.

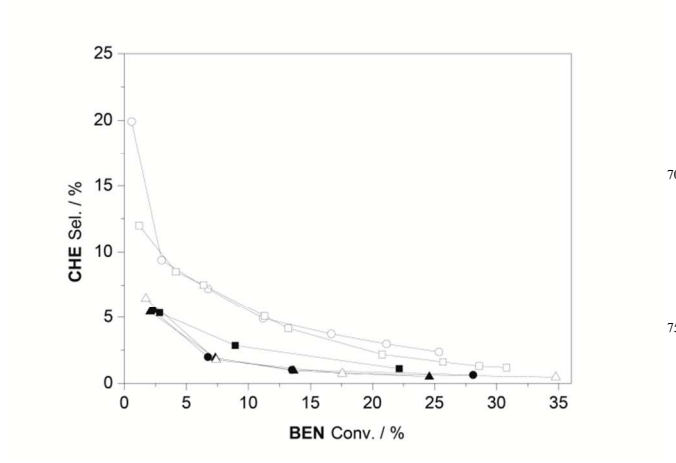

Figure 6. Cyclohexene (**CHE**) selectivity vs. benzene (**BEN**) conversion: Ru/Al_2O_3 (-●-), Ru/**B1** (-○-). Ru/**M2** (-▲-), Ru/**B2** (-Δ-), Ru/**B3** (-■-) and Ru/**B4** (-□-).

This difference can be ascribed to the effect of the nature of the IL on their supports, which is governed by (i) the nature of the lateral alkyl chain of the imidazolium cation (extension of non-polar domains) and (ii) the charge separation between the cation and the anion. The polar character of the IL increases as the charge separation in the ionic pair is greater, i.e. weaker hydrogen bond between the imidazolium ring and the anion exist. Thus, in order to evaluate the polarity, it is possible to compare relative strengths of the interactions between the cation and the anion. Experimental and theoretical studies[36-40] found the following order of intrinsic hydrogen bond strength with 1-*n*-butyl-3-methylimidazolium according to the anion: $Cl^- > CF_3CO_2^- > BF_4^- > PF_6^- > NTf_2^- > BPh_4^-$. This is indeed the inverse of the activity order observed in our experiments. Less polar hydrophobic IL-modified supports yielded more active catalysts probably due to its affinity to the apolar substract (benzene). The increase in activity observed when the side alkyl chain of imidazolium changes from methyl to *n*-butyl is in accordance with this the polarity effect on the catalytic behaviour.

Concerning the selectivity, an inverse order is observed, i.e. more polar hydrophilic IL display higher selectivities towards the olefin. It is known that ILs enhance the cyclohexene formation under biphasic conditions due to its lower solubility with respect to benzene[32] as well as by binding to the metal surface[34, 35]. The results presented herein suggest that these effects can be achieved by using SILP systems with a hydrophilic character.

In order to study the effect of the distinct IL distribution onto the Al_2O_3 on the catalytic performance, experiments were carried out using the Ru/Al_2O_3 catalyst simply impregnated with common 1-*n*-butyl-3-methyl-imidazolium ILs. Interestingly, results revealed that much lower activities were achieved with the addition of both $BMI.NTf_2$ and $BMI.PF_6$ to the non-modified support compared to Ru/**B2** and Ru/**B3**, (Table 3, Entries 2 *vs.* 7 and 4 *vs.* 8), whereas similar values of TOF were obtained in the case of Ru/Al_2O_3 impregnated with $BMI.BF_4$ and Ru/**B4** (Table 3, Entries 6 *vs.* 9). It should be noted that **B4** support has the less uniform IL distribution onto the Al_2O_3 according to ^{29}Si NMR. This is evidence that the IL distribution achieved with the method described in this work is of fundamental importance for the performance of the catalysts.

Conclusions

In conclusion, a new series of Al_2O_3 supports modified with covalently anchored imidazolium ILs were synthesised.^{13}C NMR and IR revealed not only that the structure of the IL was stable in the Al_2O_3 support but also that the anion-exchange process was accomplished with success. N_2-physisorption analysis showed that the surface area and the pore diameter were reduced by the presence of the IL, which suggests that the IL is filling the pores. Characterisation of the obtained nanocatalysts by TEM analysis revealed the formation of small and well-dispersed nanoparticles. XRD analysis confirmed that the nanoparticles possessed the Ru(0)-hcp structure, and XPS results suggested that the Ru-NPs were preferentially deposited onto the near surfaces of the support. These nanocatalysts were tested for the hydrogenation of benzene, and it was observed that activity was higher for those supports containing more hydrophobic (apolar) ILs (TOF up to 2.73 s^{-1}). Such catalysts produced TONs as high as 27000. Additionally, the cyclohexene selectivity as a function of the benzene conversion was monitored and it was observed that the selectivity (up to 20% at 1% benzene conversion) was higher for catalysts whose supports contain a more hydrophilic (polar) IL. Finally, it should be remarked that the use of Al_2O_3 supports modified with covalently anchored ILs is more suitable for catalytic applications with respect to simple impregnation with ILs, since much lower activities are observed for the latter case, in which IL is not well dispersed onto the support. The catalytic behaviours observed highly suggest that, by using these procedures, it is possible to obtain nanocatalysts with thin layers of ILs surrounding/interacting with the nanoparticle surface, which modifies the performance of these catalysts.

Experimental Part

General Methods

All syntheses were performed using standard Schlenk techniques under argon atmosphere. CH_3CN and CH_2Cl_2 were purified by standard procedures.[41] The Al_2O_3 used in this study was provided by Petrobras. Bis(2-methylallyl)(1,5-cyclooctadiene)ruthenium(II) ($Ru(Me\text{-}allyl)_2(COD)$) was purchased from Sigma-Aldrich. The IL 1-methyl-3-(trimethoxysilylpropyl)-imidazolium chloride (**1**) and 1-*n*-butyl-3-(trimethoxysilylpropyl)-imidazolium chloride (**2**) was prepared by a previously described procedure.[25] H_2 (> 99.999%) was purchased from White-Martins. Elemental analysis of the ILs immobilised on the support surfaces was carried out on a CHN Perkin Elmer M CHNS/O Analyzer, model 2400. The N_2 isotherms of the supports, previously degassed at 100°C under vacuum for 3 h, were obtained using a Tristar 3020 Micromeritics

equipment. The specific surface areas were determined by the BET multipoint method and the average pore size was obtained by BJH method. Solid-state ^{13}C and ^{29}Si NMR measurements for the supports were performed on a Bruker 400 spectrometer at the Universidade Nova de Lisboa. The infrared spectra were obtained on an ABB FTLA 2000 with a resolution of 4 cm^{-1}, with 128 cumulative scans. TEM samples were prepared by the slow evaporation of a drop of each colloidal solution deposited under an argon atmosphere onto a holey carbon-covered copper grid. The Dark Field TEM experiments were performed with a JEOL – JEM 1200ExII electron microscope operating at 200 kV. The Ru content was determined by X-ray fluorescence (XRF) carried out using a Shimadzu XRF-1800 sequential X-ray fluorescence spectrometer. Samples were prepared in KBr and calibration was performed using bromine as an internal standard. X-ray diffraction (XRD) analyses were carried out using a Philips X'Pert MPD diffractometer with Bragg-Brentano geometry using a graphite curved-crystal with the Cu Kα X-ray radiation (1,5406 Å). X-ray photoelectron spectroscopy (XPS) experiments were carried out in a conventional electron spectrometer (Omicron) equipped with a high performance hemispherical energy analyser with a seven channeltron detector. Mg X-ray source (Mg $K\alpha_{1,2}$ =1253.6 eV) was used as excitation source and the Al 2p signal at 74.5 eV was taken as reference peak.[42, 43] Analysis of the Ru, C, Al and Cl envelopes was performed and peak-fitted after subtraction of a Shirley background using Gaussian–Lorenzian peak shapes obtained from the Casa XPS software package.

Synthesis of the covalently supported ILs M1–M4 and B1-B4:

1-methyl-3-(trimethoxysilylpropyl)-imidazolium chloride (**1**) or 1-*n*-butyl-3-(trimethoxysilylpropyl)-imidazolium chloride (**2**) (3.56 mmol) were dissolved in dry CH_3CN (25 mL) and added to 5.0 g of dried alumina. The suspension was kept at 90°C under argon and vigorously stirred for 72 h. The IL-functionalised alumina was washed, centrifuged, and dried to yield the support **M1** and **B1**, respectively. Based on the amount of IL on the **M1** and **B1** support, an excess (1.2 eq.) of $LiNTf_2$, KPF_6, and $NaBF_4$ salts was dissolved in deionised water (25 mL) and added to the **M1** or **B1** (1.0 g) in order to exchange the ions. The suspensions were vigorously stirred for 48 h. The mixtures were washed, centrifuged, and dried to yield the supports **M2**-**M4** and **B2**-**B4**. The removal of chlorides from the support was checked by analysing the Cl^- content of the washing fractions by titration with $AgNO_3$.

Sputtering deposition of Ru-NPs:

As a general procedure, the appropriate Al_2O_3 support (1.0 g) was placed in a conical Al flask inside a vacuum chamber. The chamber was closed and its pressure lowered to a base pressure of 4 μbar. The support was then evacuated for 4 h, after which the vacuum chamber was placed under a sputtering working pressure of 4 mbar by adding Ar flow. The supports were continuously homogenised by revolving the Al flask at a frequency of 24 Hz. The Ru was sputtered onto the revolving support at 145 W for 10 min. After the deposition, the chamber was vented with N_2 and the grey powder was recovered and stored under Ar for their further characterisation and application.

Details about the chamber containing an electro-magnetic oscillator (with variable controlled frequency) which allows the constant movement of the conical flask are described elsewhere.[12, 44]

Hydrogenation of benzene:

2.64 g of benzene (**BEN**) (34 mmol) were added to a Fischer-Porter reactor containing the 50 mg of the Ru-nanocatalyst. After that, the reactor was pressurized with 4 bar of H_2 at the desired temperature. Samples were taken from the reaction mixture at regular intervals. The conversion and selectivity was determined by GC-FID analysis using an Agilent Technologies GC System 6820 with a DB-17 column (oven temperature 40°C).

Notes and references

[a] *Institute of Chemistry, UFRGS, Avenida Bento Gonçalves, 9500, Porto Alegre 91501-970 RS, Brazil. Fax: (+55) 5133087304; E-mail: jairton.dupont@ufrgs.brAddress.*
[b] *Institute of Physics, UFRGS, Avenida Bento Gonçalves, 9500, Porto Alegre 91501-970 RS, Brazil.*
[c] *School of Chemistry, University of Nottingham, University Park, Nottingham, NG7 2RD, UK*
Jairton.dupont@nottingham.ac.uk

† Electronic Supplementary Information (ESI) available: [Figure 1S and 2S show TGA analysis profiles for supports and description of a general procedure for the synthesis of supported Ru-NPs from Ru(Me-allyl)$_2$(COD)]. See DOI: 10.1039/b000000x/

‡ Footnotes should appear here. These might include comments relevant to but not central to the matter under discussion, limited experimental and spectral data, and crystallographic data.

1. D. Astruc, *Nanoparticles and Catalysis*, Wiley, Weinheim, 2008.
2. D. Astruc, F. Lu and J. R. Aranzaes, *Angew. Chem. Int. Ed.*, 2005, **44**, 7852-7872.
3. L. Luza, A. Gual and J. Dupont, *ChemCatChem*, 2014, **6**, 702-710.
4. A. Gual, C. Godard, S. Castillon and C. Claver, *Dalton Trans.*, 2010, **39**, 11499-11512.
5. N. Yan, C. X. Xiao and Y. Kou, *Coord. Chem. Rev.*, 2010, **254**, 1179-1218.
6. J. D. Scholten, B. C. Leal and J. Dupont, *ACS Catal.*, 2012, **2**, 184-200.
7. C. Vollmer and C. Janiak, *Coord. Chem. Rev.*, 2011, **255**, 2039-2057.
8. A. Gual, C. Godard, S. Castillón, D. Curulla-Ferré and C. Claver, *Catal. Today*, 2012, **183**, 154-171.
9. H. Wender, P. Migowski, A. F. Feil, S. R. Teixeira and J. Dupont, *Coord. Chem. Rev.*, 2013, **257**, 2468-2483.
10. H. Wender, L. F. de Oliveira, P. Migowski, A. F. Feil, E. Lissner, M. H. G. Prechtl, S. R. Teixeira and J. Dupont, *J. Phys. Chem. C*, 2010, **114**, 11764-11768.
11. H. Wender, R. V. Goncalves, A. F. Feil, P. Migowski, F. S. Poletto, A. R. Pohlmann, J. Dupont and S. R. Teixeira, *J. Phys. Chem. C*, 2011, **115**, 16362-16367.
12. R. Bussamara, D. Eberhardt, A. F. Feil, P. Migowski, H. Wender, D. P. de Moraes, G. Machado, R. M. Papaleo, S. R. Teixeira and J. Dupont, *Chem. Commun.*, 2013, **49**, 1273-1275.
13. A. Kauling, G. Ebeling, J. Morais, A. Pádua, T. Grehl, H. H. Brongersma and J. Dupont, *Langmuir*, 2013, **29**, 14301-14306.

14. L. Luza, A. Gual, D. Eberhardt, S. R. Teixeira, S. S. X. Chiaro and J. Dupont, *ChemCatChem*, 2013, **5**, 2471-2478.
15. T. Abe, M. Tanizawa, K. Watanabe and A. Taguchi, *Energy Environ. Sci.*, 2009, **2**, 315-321.
16. A. S. Kashin and V. P. Ananikov, *Russ. Chem. Bull. Int. Ed.*, 2007, **60**, 2602—2607.
17. B. Liu, L. Wen and X. Zhao, *Sol. Energ. Mat. Sol. C.*, 2008, **92**, 1-10.
18. L. Luza, A. Gual, C. P. Rambor, D. Eberhardt, S. R. Teixeira, F. Bernardi, D. L. Baptista and J. Dupont, *Phys. Chem. Chem. Phys.*, 2014, **16**, 18088-18091.
19. J. Dupont, *Acc. Chem. Res.*, 2011, **44**, 1223-1231.
20. P. Migowski and J. Dupont, *Chem. Eur. J.*, 2007, **13**, 32-39.
21. M. Jakuttis, A. Schönweiz, S. Werner, R. Franke, K.-D. Wiese, M. Haumann and P. Wasserscheid, *Angew. Chem. Int. Ed.*, 2011, **50**, 4492-4495.
22. C. P. Mehnert, *Chem. Eur. J.*, 2005, **11**, 50-56.
23. C. P. Mehnert, E. J. Mozeleski and R. A. Cook, *Chem. Commun.*, 2002, **0**, 3010-3011.
24. A. Riisagera, R. Fehrmanna, M. Haumannb and P. Wasserscheidb, *Top. Catal.*, 2006, **40**, 91-102.
25. Y. S. Chi, J. K. Lee, S.-g. Lee and I. S. Choi, *Langmuir*, 2004, **20**, 3024-3027.
26. T. Buffeteau, J. Grondin and J. C. Lassègues, *Appl. Spectrosc.*, 2010, **64**, 112-119.
27. T. Buffeteau, J. Grondin, Y. Danten and J.-C. Lassègues, *J. Phys. Chem. B*, 2010, **114**, 7587-7592.
28. L. Wang, S. Shylesh, D. Dehe, T. Philippi, G. Dörr, A. Seifert, Z. Zhou, M. Hartmann, R. N. Klupp Taylor, M. Jia, S. Ernst and W. R. Thiel, *ChemCatChem*, 2012, **4**, 395-400.
29. M. Pursch, R. Brindle, A. Ellwanger, L. C. Sander, C. M. Bell, H. Händel and K. Albert, *Solid State Nucl. Magn. Reson.*, 1997, **9**, 191-201.
30. S. Steudte, J. Neumann, U. Bottin-Weber, M. Diedenhofen, J. Arning, P. Stepnowski and S. Stolte, *Green Chem.*, 2012, **14**, 2474-2483.
31. L. Rodriguez-Perez, Y. Coppel, I. Favier, E. Teuma, P. Serp and M. Gomez, *Dalton Trans.*, 2010, **39**, 7565-7568.
32. E. T. Silveira, A. P. Umpierre, L. M. Rossi, G. Machado, J. Morais, G. V. Soares, I. J. Baumvol, S. R. Teixeira, P. F. Fichtner and J. Dupont, *Chem. Eur. J.*, 2004, **10**, 3734-3740.
33. A. P. Umpierre, E. de Jesús and J. Dupont, *ChemCatChem*, 2011, **3**, 1413-1418.
34. F. Schwab, M. Lucas and P. Claus, *Angew. Chem. Int. Ed.*, 2011, **50**, 10453-10456.
35. F. Schwab, M. Lucas and P. Claus, *Green Chem.*, 2013, **15**, 646-649.
36. F. C. Gozzo, L. S. Santos, R. Augusti, C. S. Consorti, J. Dupont and M. N. Eberlin, *Chem. Eur. J.*, 2004, **10**, 6187-6193.
37. P. A. Hunt, B. Kirchner and T. Welton, *Chem. Eur. J.*, 2006, **12**, 6762-6775.
38. C. S. Consorti, P. A. Z. Suarez, R. F. de Souza, R. A. Burrow, D. H. Farrar, A. J. Lough, W. Loh, L. H. M. da Silva and J. Dupont, *J. Phys. Chem. B*, 2005, **109**, 4341-4349.
39. P. A. Hunt and I. R. Gould, *J. Phys. Chem. A*, 2006, **110**, 2269-2282.
40. S. Tsuzuki, H. Tokuda and M. Mikami, *Phys. Chem. Chem. Phys.*, 2007, **9**, 4780-4784.
41. W. L. F. Armarego and D. D. Perrin, *Purification of Laboratory Chemicals,* 4th edn., Butterworth-Heineman, Oxford (UK), 1997.
42. V. Mazzieri, F. Coloma-Pascual, A. Arcoya, P. L'Argentiere and N. S. Figoli, *Appl. Surf. Sci.*, 2003, **210**, 222-230.
43. V. A. Mazzieri, P. C. L'Argentiere, F. Coloma-Pascual and N. S. Figoli, *Ind. Eng. Chem. Res.*, 2003, **42**, 2269-2272.
44. J. Dupont, A. F. Feil, P. Migowski, D. Eberhardt, S. R. Teixeira, P. E. G. C. Silva and J. V. Gonçalves,UFRGS*, Brazil Pat.*, 2012.

Ruthenium nanoparticles obtained by sputtering deposition from bulk metal onto an ionic-liquid modified alumina are highly active catalysts for the hydrogenation of benzene.